

Lift-off protocols for thin films for use in EXAFS experiments

S. Decoster,^{a,b*} C. J. Glover,^c B. Johannessen,^c R. Giulian,^d D. J. Sprouster,^b P. Kluth,^b L. L. Araujo,^d Z. S. Hussain,^e C. Schnorr,^f H. Salama,^b F. Kremer,^b K. Temst,^a A. Vantomme^a and M. C. Ridgway^b

^aInstituut voor Kern- en Stralingsfysica, KU Leuven, Celestijnenlaan 200D, 3001 Leuven, Belgium, ^bAustralian National University, Research School of Physics and Engineering, Canberra, ACT 0200, Australia, ^cAustralian Synchrotron, Clayton, VIC 3168, Australia, ^dUniversidade Federal do Rio Grande do Sul, Porto Alegre, Brazil, ^eCSIRO Process Science and Engineering, Clayton South, VIC 3169, Australia, and ^fInstitut für Festkörperphysik, Friedrich-Schiller-Universität Jena, Max-Wien-Platz 1, 07743 Jena, Germany. E-mail: stefan.decoster@fys.kuleuven.be

Lift-off protocols for thin films for improved extended X-ray absorption fine structure (EXAFS) measurements are presented. Using wet chemical etching of the substrate or the interlayer between the thin film and the substrate, stand-alone high-quality micrometer-thin films are obtained. Protocols for the single-crystalline semiconductors GeSi, InGaAs, InGaP, InP and GaAs, the amorphous semiconductors GaAs, GeSi and InP and the dielectric materials SiO₂ and Si₃N₄ are presented. The removal of the substrate and the ability to stack the thin films yield benefits for EXAFS experiments in transmission as well as in fluorescence mode. Several cases are presented where this improved sample preparation procedure results in higher-quality EXAFS data compared with conventional sample preparation methods. This lift-off procedure can also be advantageous for other experimental techniques (e.g. small-angle X-ray scattering) that benefit from removing undesired contributions from the substrate.

Keywords: EXAFS; thin film; lift-off; semiconductor; dielectric.

1. Introduction

In many technological applications the use of micrometer and even nanometer thin films has become standard practice. However, a detailed structural characterization of such films can be complicated by unwanted contributions from the substrate. One example of such a characterization technique, where the presence of the substrate is undesirable, is extended X-ray absorption fine structure (EXAFS) spectroscopy.

The two main measurement modes of an EXAFS experiment are transmission and fluorescence.¹ In *transmission* mode, the X-ray absorption coefficient (E) is determined by directly comparing the number of incident and transmitted photons. This mode is typically used when the relative concentration of the element of interest is several percent or more. The optimum sample thickness t satisfies $\mu(E)t \approx 2$ above the absorption edge, with the edge step $\Delta\mu(E)t \approx 1$. Homogeneity, planarity and the absence of pinholes and voids are additional prerequisites for accurate measurements. If these sample conditions can be met, transmission EXAFS is straightforward and the preferred measurement mode,

yielding an improved signal-to-noise ratio compared with the fluorescence mode.

In *fluorescence* mode, the X-ray absorption coefficient is determined by comparing the number of fluorescent photons with the number of incident photons. This mode is used when the element of interest is present in low concentrations, a few atomic percent or (much) less. The fluorescent X-rays are detected in a (multi-element) solid-state detector, positioned at 90° with respect to the incident polarized X-ray beam, to minimize elastic scattering from the sample. When using fluorescence EXAFS to study a small concentration of absorbers within a thin film on a bulk substrate, the latter contributes both fluorescent, diffracted and scattered X-rays to the total signal measured by the solid-state detector.

Many of the above-mentioned issues related to EXAFS experiments can be resolved when the measurements are performed on stand-alone thin films. In this manuscript we present sample preparation protocols for a range of semiconductor and dielectric materials, based on the separation of a thin film from the underlying substrate, which we refer to as *lift-off* henceforth. This procedure yields high-quality thin films separated from the substrate by chemical etching.

Similar procedures have been used in the semiconductor industry to produce stand-alone GaAs and AlGaAs thin films

¹ A third frequently used measurement mode for EXAFS experiments, which we will not consider here, is total electron yield, where the absorption coefficient $\mu(E)$ is determined by measuring the electron yield.

(Konagai *et al.*, 1978; Yablonovitch *et al.*, 1987). Both Konagai *et al.* and Yablonovitch *et al.* utilized selective chemical etching of an Al-rich $\text{Al}_x\text{Ga}_{1-x}\text{As}$ interlayer to lift-off Ga-rich $\text{Al}_x\text{Ga}_{1-x}\text{As}$ thin films from a GaAs substrate. These studies were driven by reducing the cost of growing GaAs thin films, since the GaAs substrate could be re-used, and by reducing the weight, which is important for GaAs solar cells in space applications.

In this manuscript we show the applicability of lift-off protocols to a broad range of material systems, including elemental (Si, Ge), binary (InP , GaAs, $\text{Ge}_x\text{Si}_{1-x}$) and ternary ($\text{In}_x\text{Ga}_{1-x}\text{As}$, $\text{In}_x\text{Ga}_{1-x}\text{P}$) semiconductors in single-crystal and amorphous forms, as well as dielectric materials (SiO_2 and Si_3N_4). We demonstrate the advantages of these protocols for EXAFS experiments, both in transmission and in fluorescence mode. We present four examples, including an accurate structural characterization of (i) single-crystalline materials and (ii) amorphous semiconductor materials, (iii) the structure of nanoparticles in dielectrics and (iv) the lattice location of dilute impurities in Ge and Si. These protocols are not restricted to the material systems presented here, but are generally applicable across a range of materials for which there exists appropriate chemical etching selectivity (Clawson, 2001).

2. Experimental cases

2.1. Crystalline semiconductors

Determining the structural parameters of bulk condensed matter with EXAFS can be performed in transmission mode, by grinding the material of interest to a fine powder which is then mixed with a binding agent such as boron nitride or cellulose to achieve the optimal sample thickness. However, many materials such as binary (GeSi, AlN, GaN, InN, ...) and ternary (InGaAs, InGaP, InGaN, ...) semiconductors are utilized in thin film form, grown on a bulk substrate. A structural characterization of these materials with EXAFS without further sample processing requires fluorescence experiments. Here, we present lift-off protocols for several single-crystal semiconductor thin films (GeSi, InGaAs, InGaP and InP), which enable transmission EXAFS experiments of superior accuracy. This method is particularly useful when the thin film and substrate contain common elements, such as lattice-matched InGaP on GaAs or InGaAs on InP. Clearly, the contribution from the substrate is negated after the thin film lift-off.

A schematic representation of the sample preparation procedure for single-crystal $\text{Ge}_x\text{Si}_{1-x}$ thin films is shown in Fig. 1(a). Thin films of $\text{Ge}_x\text{Si}_{1-x}$ are deposited on silicon-on-insulator substrates by molecular beam epitaxy (MBE). The surface is masked with Apiezon black wax² and placed in an

HF:H₂O (1:2) solution for 48 h to dissolve the SiO_2 without affecting the $\text{Ge}_x\text{Si}_{1-x}$ thin film or the Si substrate. The Si substrate is thus removed and the $\text{Ge}_x\text{Si}_{1-x}$ remains attached to the thin Si interlayer and is supported by the black wax. The black wax is then removed with trichloroethylene (TCE), the lift-off layer is crushed to a fine powder, mixed with a binding agent and finally is supported between adhesive Kapton. Alternatively, the film can be attached to Kapton prior to removing the black wax to retain its single-crystalline form. Multiple films, on Kapton, can then be stacked together to obtain the optimum sample thickness. The thin Si layer, still attached to the $\text{Ge}_x\text{Si}_{1-x}$ thin film, yields negligible attenuation during Ge *K*-edge EXAFS experiments.³

Similar lift-off protocols for single-crystalline $\text{In}_x\text{Ga}_{1-x}\text{As}$, $\text{In}_x\text{Ga}_{1-x}\text{P}$ and InP thin films are represented schematically in Figs. 1(b), 1(c) and 1(d), respectively, and an overview of all elaborated protocols is shown in Table 1.

The lift-off protocols for GeSi, InGaP and InP described above have made it possible to determine the structural parameters of these compounds with EXAFS in transmission mode (Ridgway *et al.*, 1998b, 1999; Schnohr *et al.*, 2008). We have shown that it is possible to significantly improve the accuracy of the extracted parameters such as bond lengths and bond angles, with respect to conventional fluorescence EXAFS experiments (Aldrich *et al.*, 1994; Woicik *et al.*, 1998; Aubry *et al.*, 1999). The lift-off of InGaAs thin films, grown on GaAs or InP substrates, has made it possible to perform an accurate structural analysis on the In, Ga and As *K*-edges without interference from absorbers in the substrate (Hussain *et al.*, 2009).

2.2. Amorphous semiconductors

A detailed structural characterization of *amorphous* thin films with transmission EXAFS can be impeded by non-stoichiometry and inhomogeneity when amorphous films are deposited by conventional techniques (Del Cueto & Shevchik, 1978; Thèye *et al.*, 1980; Udron *et al.*, 1992). However, by using lift-off protocols for GaAs, GeSi and InP after ion irradiation-induced amorphization, as presented below, we have obtained high-quality samples with superior stoichiometry, homogeneity and continuity compared with sputtering or flash evaporation (Ridgway *et al.*, 1998a,b, 1999; Schnohr *et al.*, 2007; Glover *et al.*, 2001).

As depicted schematically in Fig. 1(e), thin films of epitaxial GaAs and AlAs have been deposited onto GaAs substrates by metal-organic chemical vapor deposition (MOCVD). The GaAs layer is then amorphized by ion irradiation with equal fluences of Ga and As to preserve stoichiometry. Several implantation energies and fluences are used to obtain a near-constant energy deposition in the GaAs layer. Samples are then placed in a HF:H₂O (1:10) solution for 48 h, to dissolve

² The black wax which is deposited prior to the etch step has a double purpose in the lift-off procedure. It serves as a support for the lift-off thin film allowing better handling during sample mounting. Moreover, its convex shape results in a force pulling the edges of the thin film away from the substrate, hence promoting the chemical etchant to undercut the thin film and speeding up the lift-off process.

³ To avoid the dangers of HF, an alternative approach is to first deposit a submicrometer layer of SiO_2 on the sample surface by plasma-enhanced chemical vapour deposition (PECVD) and then remove the Si substrate with mechanical grinding and KOH as described in §2.3. The thin layers of SiO_2 on either side of the material under study are effectively transparent for EXAFS with hard X-rays.

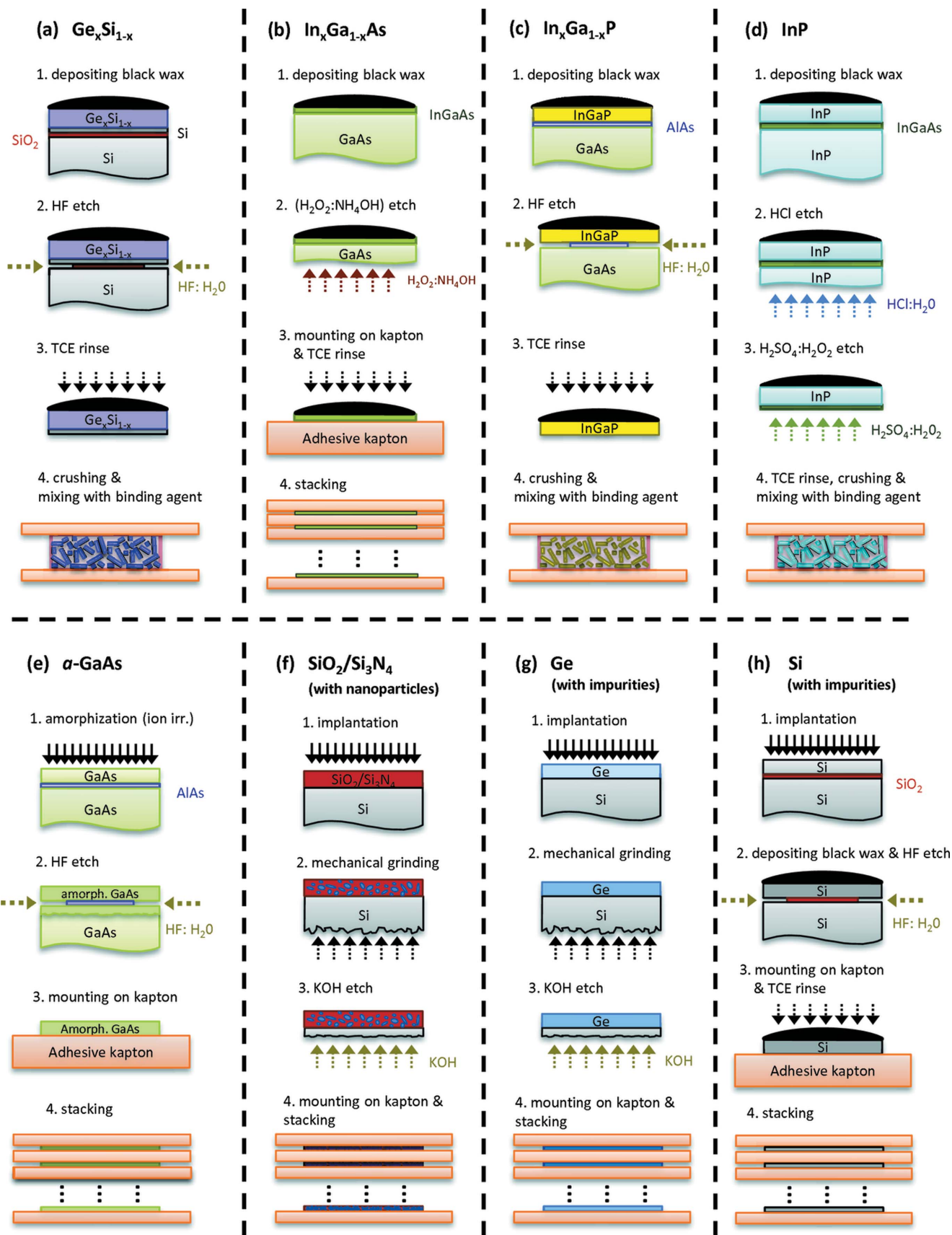


Figure 1
 (Color online) Schematic representation of the lift-off procedure for thin films of single-crystalline (a) Ge_xSi_{1-x} , (b) $In_xGa_{1-x}As$, (c) $In_xGa_{1-x}P$ and (d) InP, (e) amorphous GaAs, the dielectric materials (f) SiO_2 and Si_3N_4 embedded with nanoparticles, and single-crystalline (g) Ge and (h) Si, doped by ion implantation.

Table 1

Overview of the lift-off protocols for single-crystalline and amorphous semiconductor and dielectric thin films.

Mode	Sample	Deposition/processing	Substrate	Sacrificial layer	Etchant	Reference†
Transmission	Crystalline $\text{Ge}_x\text{Si}_{1-x}$, $0 \leq x \leq 1$	MBE	SOI	SiO_2	$\text{HF}:\text{H}_2\text{O}$	1
Transmission	Crystalline $\text{In}_x\text{Ga}_{1-x}\text{P}$, $x < 0.75$	MOCVD	GaAs	AlAs	$\text{HF}:\text{H}_2\text{O}$	2
Transmission	Crystalline InP and $\text{In}_x\text{Ga}_{1-x}\text{P}$, $x > 0.75$	MOCVD	InP	InGaAs	$\text{HCl} - \text{H}_2\text{SO}_4\ddagger$	3
Transmission	Crystalline GaAs and $\text{In}_x\text{Ga}_{1-x}\text{As}$, $x < 0.25$	MOCVD	GaAs	AlAs	$\text{HF}:\text{H}_2\text{O}$	4
Transmission	Crystalline $\text{In}_x\text{Ga}_{1-x}\text{As}$, $x > 0.25$	MOCVD	InP	Nil	HCl	4
Transmission	Amorphous group IV and III–Vs	As above + implantation	As above	As above	As above§	1, 3, 5
Fluorescence	Nanoparticles in SiO_2	Thermal oxidation + implantation	Si	Nil	KOH	6–13
Fluorescence	Nanoparticles in Si_3N_4	LPCVD + implantation	Si	Nil	KOH	
Fluorescence	Dilute impurities in Si	Implantation	SOI	SiO_2	$\text{HF}:\text{H}_2\text{O}$	
Fluorescence	Dilute impurities in Ge	MBE + implantation	Si	Nil	KOH	
Fluorescence	Dilute impurities in crystalline III–Vs	MOCVD + implantation	As above	As above	As above	

† References. 1: Ridgway *et al.* (1999); 2: Schnohr *et al.* (2008); 3: Ridgway *et al.* (1998b); 4: Hussain *et al.* (2009); 5: Schnohr *et al.* (2007); 6: Cheung *et al.* (2004); 7: Johannessen *et al.* (2005); 8: Kluth *et al.* (2006); 9: Araujo *et al.* (2006); 10: Araujo *et al.* (2008); 11: Sprouster *et al.* (2010); 12: Sprouster *et al.* (2011); 13: Giulian *et al.* (2011). ‡ HCl is used to remove the InP substrate, utilizing the InGaAs layer as an etch stop. The InGaAs layer is then removed in a $\text{H}_2\text{SO}_4:\text{H}_2\text{O}_2:\text{H}_2\text{O}$ (1:1:10) solution for ~ 5 min. § The selectivity of etchants can differ between crystalline and amorphous phases. If the selectivity is insufficient to lift off an amorphized layer, we recommend removing the film in crystalline form, van der Waals bonding to a suitable substrate, amorphizing by ion irradiation, followed by mechanical removal of the film from the substrate.

the AlAs interlayer. The amorphized GaAs layer is rinsed in H_2O , and several films are then stacked together in between Kapton to achieve the optimum thickness for EXAFS experiments at the Ga and As *K*-edges in transmission mode.

Comparable protocols can be used to obtain stand-alone thin films of amorphous GeSi and InP, using ion implantation to amorphize the thin film prior to the lift-off protocol for the single-crystalline GeSi and InP thin films, as presented in Figs. 1(c) and 1(d), respectively.

The growth of the original single-crystalline thin films is performed with MOCVD or MBE at elevated temperatures, resulting in crystalline stoichiometric layers free of pinholes and with a uniform thickness. The subsequent amorphization by ion irradiation, using multiple species with fluences proportional to the stoichiometry of the thin film, maintains the stoichiometry, continuity and thickness uniformity of the thin film. This has enabled transmission EXAFS experiments of high-quality amorphous GaAs, GeSi and InP, with superior data accuracy compared with fluorescence experiments (Ridgway *et al.*, 1998a, 1999; Schnohr *et al.*, 2007).

2.3. Nanoparticles in dielectrics

Nanoparticles receive considerable interest because of their size-dependent properties and many potential technological applications. One of the most widely applied techniques for creating embedded nanoparticles is ion implantation, followed by thermal annealing. EXAFS is an ideal technique to probe the structural and vibrational properties of nanoparticles, and, because of the relatively low concentration of the element of interest, such experiments have to be performed in fluorescence mode. The bottleneck for these experiments is the total number of absorbers in the sample, which ultimately determines the attainable *k*-range and hence the accuracy of the results. Here we will show the lift-off protocols for SiO_2 and Si_3N_4 thin films with embedded nanoparticles, as depicted in Fig. 1(f), resulting in an improved signal-to-noise ratio, hence increasing the accuracy of the parameters that are extracted from the fluorescence EXAFS experiments.

An amorphous SiO_2 or Si_3N_4 layer of roughly 2 μm is grown or deposited on a Si substrate, after which ion implantation with multiple energies (up to several MeV) and fluences is used to introduce a homogeneous distribution of the element of interest in the dielectric top layer. Thermal annealing then leads to the formation of crystalline-embedded nanoparticles. Next, the Si substrate is removed, first by mechanical grinding down to a Si thickness of 30 μm , and finally by KOH etching. The resulting thin films are then mounted on adhesive Kapton and stacked together to increase the total number of absorbers.⁴

The stacking of the nanoparticles-embedded thin SiO_2 or Si_3N_4 films results in a significantly increased fluorescence yield, while the removal of the substrate reduces the elastic scattering and avoids contributions from Bragg diffraction from the single-crystalline Si substrate. This improved signal-to-noise ratio has allowed us to study subtle differences in the structural and vibrational properties of Co, Ni, Cu, Ge, Pt and Au nanoparticles in dielectric materials with respect to their bulk structural properties (Cheung *et al.*, 2004; Johannessen *et al.*, 2005; Kluth *et al.*, 2006; Araujo *et al.*, 2006, 2008; Sprouster *et al.*, 2010, 2011; Giulian *et al.*, 2011).

The advantages of a lift-off protocol are readily demonstrated in Fig. 2 which shows EXAFS measurements in fluorescence mode for Co nanoparticles formed in SiO_2 on Si. The two samples (with and without Si substrate) were measured under identical conditions. Several artifacts due to the substrate are evident in the normalized absorbance spectrum (Fig. 2a). These include peaks due to diffraction and an enhanced yield below the edge due to leakage of scattered photons into the fluorescent region of interest. The inset compares multi-channel analyser spectra for a single detector

⁴ At X-ray energies of 8 keV or more, there is only little X-ray attenuation in the multiple layers of Kapton. Therefore, it is no problem to have a 60 μm Kapton foil for each 2 μm sample film. However, care needs to be taken when performing EXAFS experiments at lower X-ray energies (< 7 keV), because a significant fraction of the incident X-ray beam can be attenuated in the Kapton foils, hence reducing the advantage of stacking the thin films. In this case it is advised to stack all thin films together in between two adhesive Kapton foils.

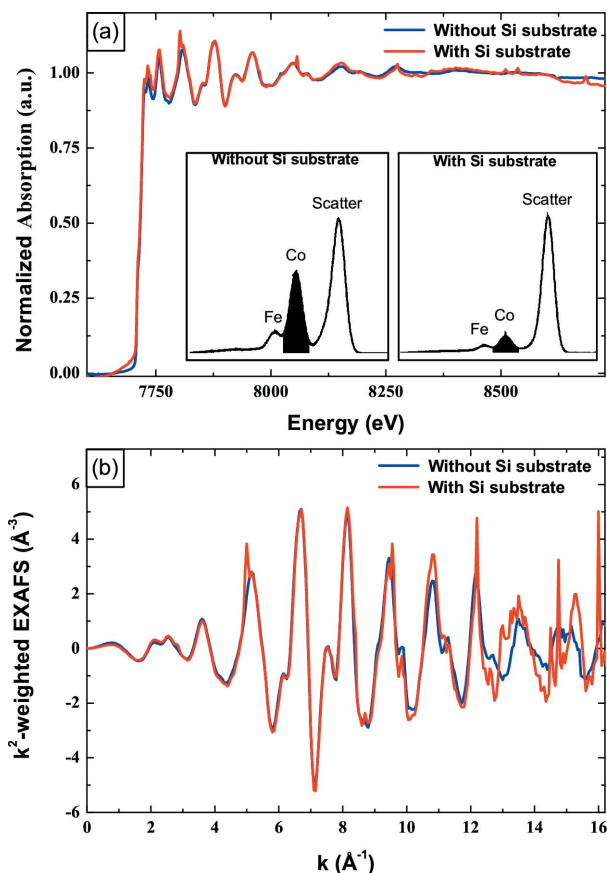


Figure 2 (Color online) Normalized absorbance spectra (a) and isolated fine structure (b) measured at the Co *K*-edge for Co nanoparticles formed in SiO₂ on Si comparing samples before and after the removal of the Si substrate. In (a) the inset compares multi-channel analyzer spectra recorded at 8 keV.

element recorded at 8 keV (the Fe contribution originates from the cryostat). With the Si substrate, the ratio of fluorescent to scattered photons is 1:10. Without the substrate, this ratio is reduced to 1:3. Furthermore, stacking the lifted-off layers produces a three- to four-fold increase in fluorescent photon yield resulting in superior data quality, particularly at high *k* values, as apparent in the comparison of the isolated fine structure (Fig. 2b).

2.4. Dilute impurities in Ge and Si

The study of the local configuration of isolated impurities in a single-crystalline environment, such as dopants in the group IV semiconductors Si and Ge, is of significant interest because the lattice location of the dopant influences the electrical properties of the doped semiconductor. Such lattice location studies in dilute systems can be performed with fluorescence EXAFS measurements, with sensitivity and poor signal-to-noise ratio as the main challenges. Using lift-off protocols, we will show that it is possible to study the lattice location of dopants in Si and Ge with concentrations as low as a few parts per million (p.p.m.).

The lift-off procedures for a doped Ge and a doped Si thin film are schematically represented in Figs. 1(g) and 1(h),

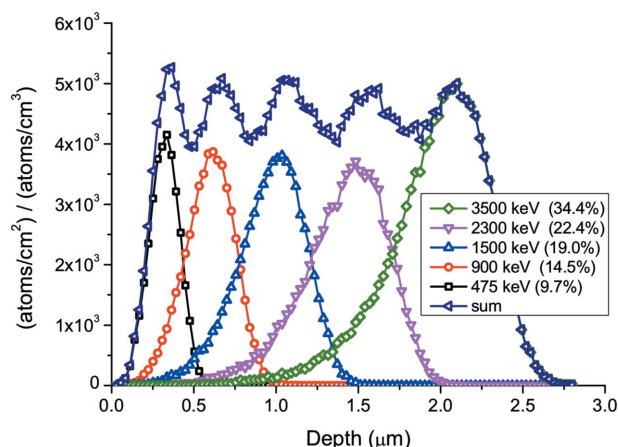


Figure 3 (Color online) Calculated As implantation profile (triangles left) into a 3 µm Si film, using five energies [3500 keV (diamonds), 2300 keV (triangles down), 1500 keV (triangles up), 900 keV (circles) and 475 keV (squares)] with relative fluences of 34.4%, 22.4%, 19.0%, 14.5% and 9.7%, respectively.

respectively. A single-crystalline Ge film of thickness 1.8 µm is grown onto a (100) Si substrate, while a 3 µm Si film is bonded on a SiO₂ film on a Si substrate with, for example, the ‘smart cut’ process (Bruel, 1996). A homogeneous distribution of dopants is achieved by implanting with multiple energies and fluences. As an example, the As implantation profile in a 3 µm Si film is shown in Fig. 3, using five energies (3500 keV, 2300 keV, 1500 keV, 900 keV and 475 keV) and relative fluences of 34.4%, 22.4%, 19.0%, 14.5% and 9.7%, respectively, as calculated by *srim2008* (Ziegler *et al.*, 1985).

All implantations are performed at an elevated temperature (523 K for Ge, 423 K for Si) to avoid amorphization of the crystalline matrix, as confirmed with Rutherford back-scattering in channeling geometry (not shown). A tilt angle of 10° with respect to the sample surface direction is used to minimize channeling during the implantation. After implantation, and, if applicable, post-implantation treatments such as thermal annealing, the top layer is removed from the substrate. By mechanical grinding, followed by KOH etching at room temperature, the Si substrate is removed from the implanted Ge thin film, after which the film is mounted on adhesive Kapton (see Fig. 1g). After the deposition of black wax, the implanted Si thin film is placed for several days in a HF:H₂O (1:10) solution, which dissolves the SiO₂ sacrificial layer.⁵ Next, the thin film is mounted on adhesive Kapton, after which the black wax is removed with TCE. Finally the lift-off implanted layers (Si and Ge), supported only by X-ray transparent Kapton, can be stacked together to increase the areal concentration of the impurities. Typically, five to ten films are stacked together, depending on the absorber/matrix combination.

⁵ To avoid the dangers of HF, an alternative approach is to first deposit a submicrometer layer of SiO₂ on the sample surface by plasma-enhanced chemical vapour deposition (PECVD) and then remove the Si substrate with mechanical grinding and KOH as described in §2.3. The thin layers of SiO₂ on either side of the material under study are effectively transparent for EXAFS with hard X-rays.

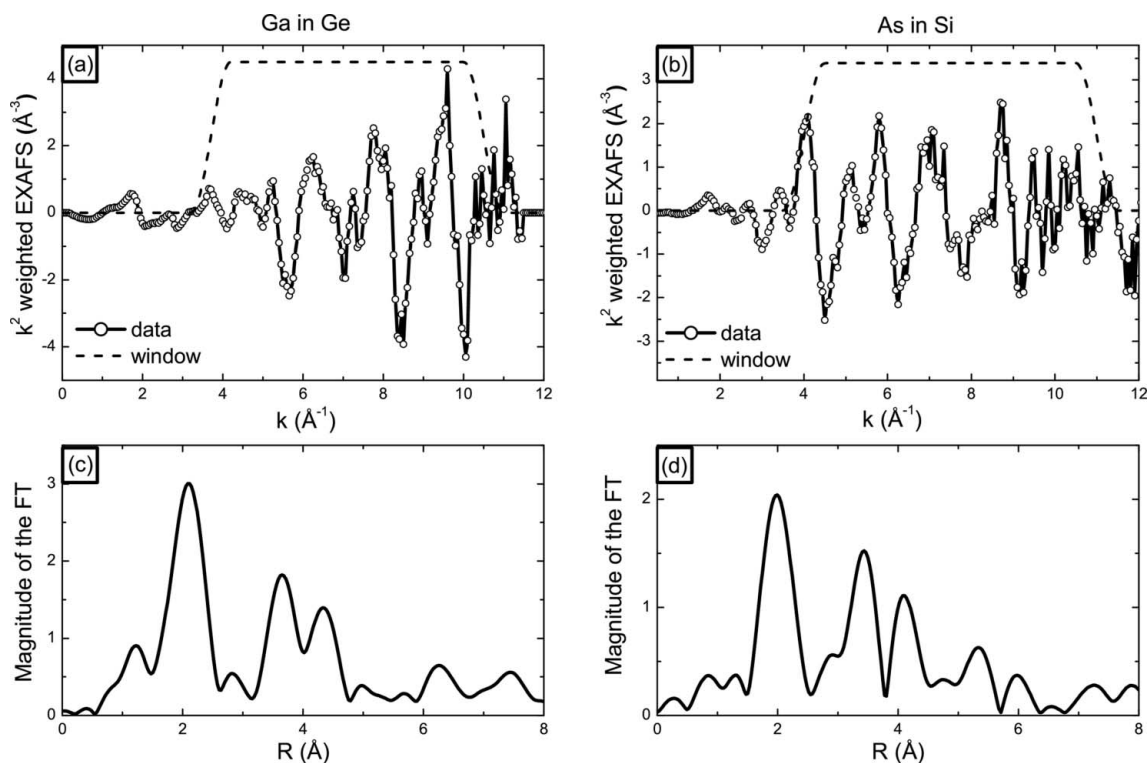


Figure 4

k^2 -weighted EXAFS spectra of (a) Ga-doped Ge and (b) As-doped Si at the Ga K -edge and As K -edge, respectively (open symbols), versus the photoelectron wavenumber k ; (c), (d) Fourier transforms of these EXAFS spectra [convoluted with a Hanning window (dashed line)] as shown in (a) and (b), respectively, as a function of the non-phase-corrected radial distance R from the absorber.

Using this lift-off protocol and a fluorescence EXAFS set-up, we were able to study the lattice location of Ga-doped Ge and As-doped Si, with concentrations as low as 2×10^{18} atoms cm^{-3} (45 p.p.m.) and 2.5×10^{17} atoms cm^{-3} (5 p.p.m.), respectively. A $Z - 1$ filter (Zn for the Ga edge, Ge for the As edge) and soller slits were positioned between the sample and the detector to reduce the elastic scattering peak and the contribution of scattered and fluorescent X-ray photons originating from the filter material.

The experimental k^2 -weighted EXAFS oscillations for the Ga-doped Ge and As-doped Si are shown in Figs. 4(a) and 4(b), respectively. These data have been obtained by averaging four measured spectra, each requiring 1 h of photon beam on target. The EXAFS oscillations, shown in Figs. 4(a) and 4(b), have been Fourier transformed and are plotted in Fig. 4(c) for Ga-doped Ge and in Fig. 4(d) for As-doped Si. A detailed analysis of the data set for Ga-doped Ge has been presented elsewhere (Decoster *et al.*, 2012). These experiments confirm that accurate lattice location studies can be performed with fluorescence EXAFS experiments, even for very low concentrations of impurities.

3. Conclusion

As apparent from these experimental examples, the lift-off protocols allow us to study the structural properties of thin films of condensed matter with EXAFS with improved accuracy, both in transmission and fluorescence mode. Moreover, in specific cases, it is the only way to obtain detailed structural

information of the material under investigation. It is clear that the lift-off technique is not limited to the materials discussed here (GeSi, InGaAs, InGaP, InP, GaAs, SiO₂, Si₃N₄, Ge and Si), but that this technique can be used to create high-quality stand-alone thin films of an even broader range of materials. The only prerequisites are the growth of a high-quality thin film on a substrate (with or without an interlayer), and a suitable etchant with an etching rate which is much higher for the substrate or the interlayer than for the thin film. While we have highlighted the strength of the lift-off technique as a sample preparation method for EXAFS experiments, it should be noted that this method can also be advantageous to other characterization techniques which suffer from unwanted substrate contributions, as has already been shown in small-angle X-ray scattering experiments (Sprouster *et al.*, 2011).

We acknowledge the support from the Research Foundation, Flanders, the Australian Research Council, the KU Leuven GOA/09/006 project, the IUAP P6/42 program and the SPIRIT (Support of Public and Industrial Research using Ion Beam Technology) project (contract No. 227012). We would like to thank the epi team of imec Belgium for the growth of the Ge on Si samples. This research was undertaken on the XAS beamline at the Australian Synchrotron, Victoria, Australia.

References

- Aldrich, D. B., Nemanich, R. J. & Sayers, D. E. (1994). *Phys. Rev. B*, **50**, 15026–15033.

- Araujo, L. L., Giulian, R., Sprouster, D. J., Schnohr, C. S., Llewellyn, D. J., Kluth, P., Cookson, D. J., Foran, G. J. & Ridgway, M. C. (2008). *Phys. Rev. B*, **78**, 094112.
- Araujo, L. L., Kluth, P., Azevedo, G., de M., & Ridgway, M. C. (2006). *Phys. Rev. B*, **74**, 184102.
- Aubry, J. C., Tyliczszak, T., Hitchcock, A. P., Baribeau, J.-M. & Jackman, T. E. (1999). *Phys. Rev. B*, **59**, 12872–12883.
- Bruel, M. (1996). *Nucl. Instrum. Methods Phys. Res. B*, **108**, 313–319.
- Cheung, A., de M. Azevedo, G., Glover, C. J., Llewellyn, D. J., Elliman, R. G., Foran, G. J. & Ridgway, M. C. (2004). *Appl. Phys. Lett.* **84**, 278.
- Clawson, A. R. (2001). *Mater. Sci. Eng.* **31**, 1–438.
- Decoster, S., Johannessen, B., Glover, C. J., Cottenier, S., Bierschenk, T., Salama, H., Kremer, F., Temst, K., Vantomme, A. & Ridgway, M. C. (2012). *Appl. Phys. Lett.* **101**, 261904.
- Del Cueto, J. A. & Shevchik, N. J. (1978). *J. Phys. C*, **11**, L829.
- Giulian, R., Araujo, L. L., Kluth, P., Sprouster, D. J., Schnohr, C. S., Byrne, A. P. & Ridgway, M. C. (2011). *J. Phys. D*, **44**, 155402.
- Glover, C. J., Ridgway, M. C., Desnica-Frankovic, I. D., Yu, K. M., Foran, G. J., Clerc, C., Hansen, J. L. & Nylandsted-Larsen, A. (2001). *Phys. Rev. B*, **61**, 073204.
- Hussain, Z. S., Wendler, E., Wesch, W., Foran, G. J., Schnohr, C. S., Llewellyn, D. J. & Ridgway, M. C. (2009). *Phys. Rev. B*, **79**, 085202.
- Johannessen, B., Kluth, P., Glover, C. J., de M., Azevedo, G., Llewellyn, D. J., Foran, G. J. & Ridgway, M. C. (2005). *J. Appl. Phys.* **98**, 024307.
- Kluth, P., Johannessen, B., Foran, G. J., Cookson, D. J., Kluth, S. M. & Ridgway, M. C. (2006). *Phys. Rev. B*, **74**, 014202.
- Konagai, M., Sugimoto, M. & Takahashi, K. (1978). *J. Cryst. Growth*, **45**, 277–280.
- Ridgway, M. C., Glover, C. J., Foran, G. J. & Yu, K. M. (1998a). *J. Appl. Phys.* **83**, 4610.
- Ridgway, M. C., Glover, C. J., Tan, H. H., Clark, A., Karouta, F., Foran, G. J., Lee, T. W., Moon, Y., Yoon, E., Hansen, J. L., Nylandsted-Larsen, A., Clerc, A. & Chaumont, J. (1998b). *Mater. Res. Soc. Symp. Proc.* **524**, 309.
- Ridgway, M. C., Yu, K. M., Glover, C. J., Foran, G. J., Clerc, C., Hansen, J. L. & Nylandsted-Larsen, A. (1999). *Phys. Rev. B*, **60**, 10831–10836.
- Schnohr, C. S., Araujo, L. L., Kluth, P., Sprouster, D. J., Foran, G. J. & Ridgway, M. C. (2008). *Phys. Rev. B*, **78**, 115201.
- Schnohr, C. S., Kluth, P., Byrne, A. P., Foran, G. J. & Ridgway, M. C. (2007). *Nucl. Instrum. Methods Phys. Res. B*, **257**, 293–296.
- Sprouster, D. J., Giulian, R., Araujo, L. L., Kluth, P., Johannessen, B., Cookson, D. J., Foran, G. J. & Ridgway, M. C. (2010). *J. Appl. Phys.* **107**, 014313.
- Sprouster, D. J., Giulian, R., Araujo, L. L., Kluth, P., Johannessen, B., Kirby, N. & Ridgway, M. C. (2011). *J. Appl. Phys.* **109**, 113517.
- Thèye, M.-L., Gheorghiu, A. & Launois, H. (1980). *J. Phys. C*, **13**, 6569.
- Udron, D., Flank, A.-M., Lagarde, P., Raoux, D. & Thèye, M.-L. (1992). *J. Non-Cryst. Solids*, **150**, 361–365.
- Woicik, J. C., Miyano, K. E., King, C. A., Johnson, R. W., Pellegrino, J. G., Lee, T. L. & Lu, Z. H. (1998). *Phys. Rev. B*, **57**, 14592–14595.
- Yablonovitch, E., Gmitter, T., Harbison, J. P. & Bhat, R. (1987). *Appl. Phys. Lett.* **51**, 2222.
- Ziegler, J., Biersack, J. & Littmark, U. (1985). *The Stopping and Range of Ions in Solids*. New York: Pergamon Press.